Int. J. Heat Mass Transfer. Vol. 35, No. 8, pp. 1893–1904, 1992
Printed in Great Britain

0017-9310/92 $5.00 + 0.00

Nucleate pool boiling data for five refrigerants on plain, integral-fin and enhanced tube geometries

RALPH L. WEBB and CHRISTOPHER PAIS
Department of Mechanical Engineering, The Pennsylvania State University, University Park, PA 16802, U.S.A.

(*Received* 3 *January* 1991 *and in final form* 13 *August* 1991)

Abstract—Data are presented for nucleate pool boiling on five different horizontal tube geometries using five refrigerants at two saturation temperatures. The refrigerants tested are R-11, R-12, R-22, R-123 and R-134a at saturation temperatures of 4.44°C (40°F) and 26.7°C (80°F). The tube geometries tested are a plain tube, a 1024 fins/m integral-fin tube, and three commercially used enhanced tube geometries (GEWA TX19, GEWA SE, and Turbo-B). The wide range of data reported here is new to the literature. The ability of the Cooper and the Stephan–Abdelsalam correlations to predict the plain tube data is evaluated. The slopes of the boiling coefficient vs heat flux curve are found to be heat flux dependent. Of particular importance are the data on R-123 and R-134a, which are intended to replace R-11 and R-12, respectively. Except for the Turbo-B with R-11, it appears that the boiling coefficients for R-123 and R-134a are within 10% of the values for R-11 and R-12, respectively.

INTRODUCTION

NUCLEATE boiling is an important mode of heat transfer, and it is used on the shell side of tubular heat exchangers in the refrigeration and process industries. In the refrigeration industry, it is used in flooded refrigerant evaporators, where a refrigerant boils on the outside of a tube bundle, thereby cooling the tube side fluid. In order to predict the performance of these evaporators, one needs to know the heat transfer coefficient on the shell side.

The shell side boiling mechanism is one of combined nucleate boiling and forced convection vaporization. One may predict the forced convection shell side heat transfer coefficient using a forced convection boiling model, such as that proposed by Chen [1]. The Chen model is given by

$$h_o = Sh_{nb} + Fh_{fc}. \quad (1)$$

The first and second terms on the right hand side of equation (1) account for the nucleate boiling, and the two-phase forced convection contributions to the refrigerant boiling coefficient, respectively. The term h_{nb} is for nucleate pool boiling on a single tube of the geometry of interest. The h_{nb} term may be written as a funcion of $\Delta T_{ws}(= T_w - T_s)$, or alternatively, as a function of heat flux, q_{nb}/A. The term h_{fc} is the single-phase forced convection coefficient for the liquid phase flowing alone in the bundle. The suppression factor (S) and the forced convection multiplier (F) are functions of two-phase flow parameters. Correlations are necessary for calculation of the four component terms in equation (1). The F-term is a function of the 'two-phase friction multiplier', ϕ_f^2, which relates to the two-phase friction pressure gradient.

Webb *et al.* [2, 3] and Webb and Apparao [4] used equation (1) to predict the performance of an R-11 chiller having integral-fin tubes. Figures 1(b)–(d) show tube geometries typically used in flooded refrigerant evaporators. Figure 1(a) is the integral-fin tube, whose chiller performance was predicted by Webb *et al.* [2, 3]. Figures 1(c)–(d) are 'enhanced' tube geometries, which provide much higher performance than the plain tube, or the integral-fin tube.

Flooded refrigerant evaporators are typically designed for use with any of the following refrigerants: R-11, R-12, R-22, and R-113. However, concern over ozone depletion in the stratosphere, caused by chlorine in these refrigerants, has resulted in an international commitment to discontinue the use of R-11, R-12 and R-113. The ozone layer acts as a protective blanket that shields against the harmful ultra-violet radiation emitted by the sun. The United Nations 'Montreal Protocol' [5] describes a proposal to reduce the production and use of refrigerants that have an ozone depletion potential. Alternative refrigerants with lower ozone depletion potential have been developed to replace R-11 and R-12. Refrigerants R-123 and R-134a are the proposed replacements for R-11 and R-12, respectively.

Prediction of the chiller performance requires knowledge of the nucleate boiling heat transfer coefficient, h_{nb}, for the tube geometries and refrigerants of interest. Except for plain tubes, no correlations exist for predicting h_{nb} as a function of temperature and refrigerant type for any of the Fig. 1 surface geometries. Hence, it is necessary to have actual pool boiling data for the refrigerant of interest, at the evaporator operating temperature, for use of equation (1). Since water chiller evaporators typically operate at refrigerant temperatures of 35°F (2°C), or below, pool boiling data are required for the range

NOMENCLATURE

A	heat transfer area based on envelope diameter
D_o	envelope diameter of the tube
F	factor in Chen model, equation (1)
h_{fc}	shell side heat transfer coefficient for liquid phase alone
h_{nb}	single-tube pool boiling coefficient based on A_o
h_o	composite shell side heat transfer coefficient
p	saturation pressure
p_{cr}	critical pressure
p_r	p/p_{cr}
q_{nb}	heat transfer rate for nucleate boiling
q''	heat flux, q_{nb}/A
S	suppression factor in Chen model
T	temperature: T_s, refrigerant saturation temperature; T_w, wall temperature
ΔT_{ws}	$T_w - T_s$.

Greek symbols

θ	angular position from the vertical (zero at the top of the tube)
ϕ_f^2	two-phase frictional multiplier.

Subscripts

fc	single-phase forced convection
nb	single-tube nucleate boiling
o	outside
s	saturation temperature
w	wall, at the base of the fins.

$14 < T_s < 40°F (-10 < T_s < 4°C)$. The literature survey of Pais and Webb [6] shows that a considerable amount of published data exists on nucleate boiling of refrigerants. However, much of the data have been taken with R-113 or R-11 at one atmosphere, for which the saturation temperature is 80°F (27°C) or higher. Literally no data have been published for the new refrigerants, R-123 and R-134a. Hence, the state of published knowledge to predict the performance of flooded refrigerant evaporators for tube geometries and refrigerants is virtually nonexistent.

The overall purpose of the authors' work is to develop design correlations for the tube geometries and refrigerants of interest. Before this can be done, a database of nucleate boiling data is necessary. This paper presents boiling data which have been taken to provide the required database.

TUBE GEOMETRIES TESTED

Saturated nucleate boiling data were taken on a plain tube and the four tube geometries illustrated in Fig. 1. The geometry details of these tubes are given in Table 1. Tests were performed at two saturation temperatures, 4.44°C (40°F) and 26.7°C (80°F) using refrigerants R-11, R-12, R-22, R-123 and R-134a. The Fig. 1 tubes were made by commercial tube manufacturers. However, the present tubes were specially made to have a 9.53 mm smooth inside bore. This was done to facilitate wall thermocouple and electric cartridge heater installation.

EXPERIMENTAL APPARATUS

The single-tube pool boiling apparatus consists of a cylindrical boiling cell made of copper with a diameter of 76.2 mm (3 in.) and a length of 177.8 mm (7 in.) as shown in Fig. 2. The tube specimen is soldered to a flange at one end of the cylinder. The other end of the cylinder consists of a tempered sight glass to observe the boiling and to check the liquid level.

Each tube has two internal, axial grooves machined diametrically opposite and are used for thermocouple installation as shown in Fig. 3. The grooves are along the total tube length, and were machined by electrostatic discharge machining (EDM). The tube is soldered to a brass flange, which can rotate inside an annular brass flange. An O-ring seals between the two flanges. The rotation of the inner flange relative to the outer flange allows checking of the consistency of the temperatures indicated by the two wall thermocouples.

The copper tubes were 17.5–19.1 mm in diameter over the fins, with an inner diameter of 9.53 mm. Electric cartridge heaters 152.4 mm long and 9.53 mm in diameter with a maximum power output of 500 W are inserted in copper tube. A sliding fit existed between the heater and the tube. Thermal contact between the heater and the tube is enhanced by applying a coat of heat-sink compound on the heater before installing it in the tube. The power supplied to the heaters is varied using an auto-transformer. A precision voltmeter and an ammeter are used to measure the input power.

Two copper–constantan thermocouples are installed in the grooves to measure the wall temperature. The thermocouple junctions are located 50 mm from the free end of the tubes. Thermocouples are also installed in the liquid pool and the vapor to measure the saturation temperature. All copper–constantan thermocouples were made from the same roll of 0.13 mm diameter wire. The thermocouples are circuited to allow direct measurement of the difference between the wall temperature and the saturation temperature (the temperature of the liquid pool). The thermocouples are connected to a thermocouple switching box, and their output is measured using a precision millivoltmeter. The directly measured

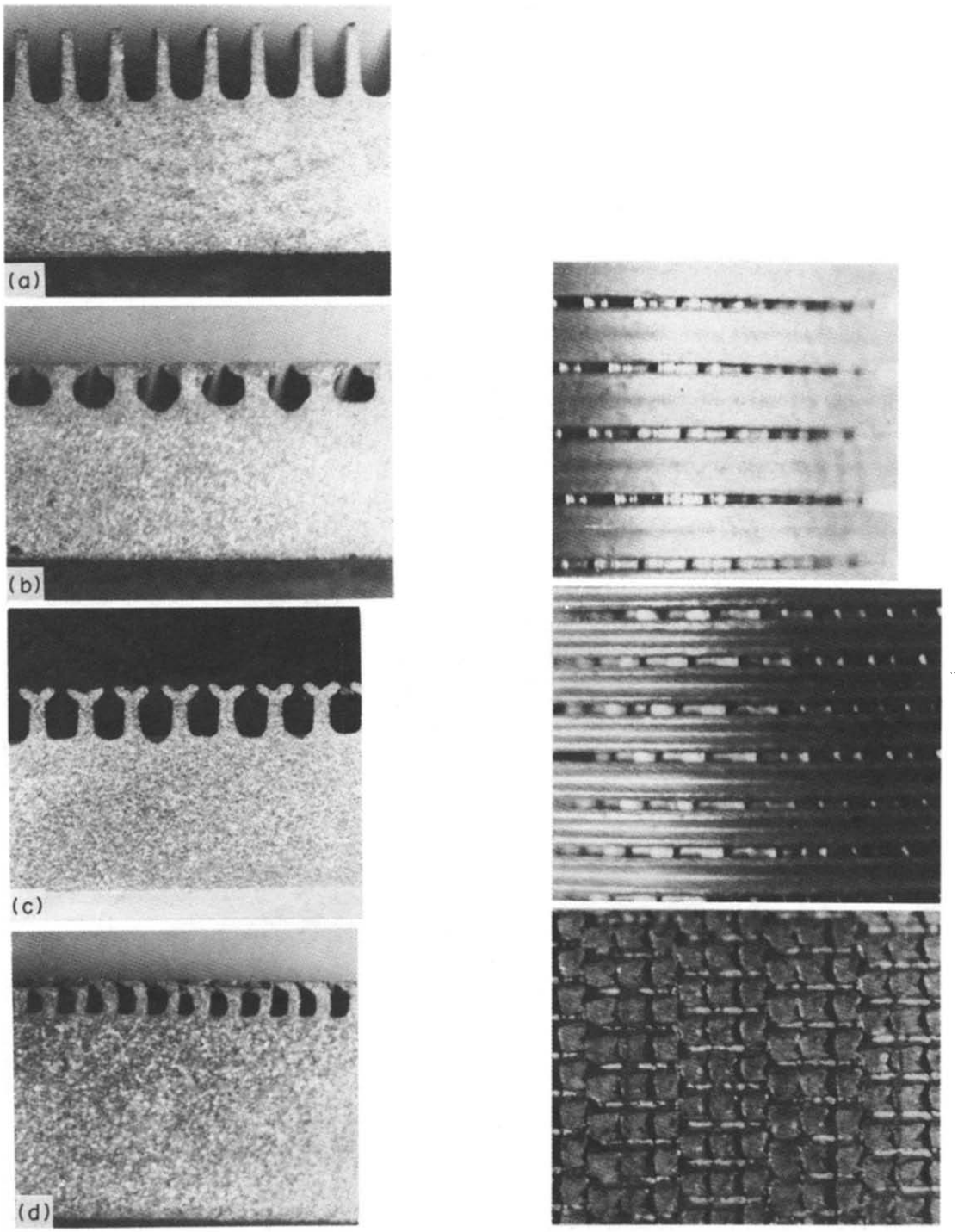

FIG. 1. Tube geometries for shell side nucleate boiling: (a) GEWA K26; (b) GEWA TX19; (c) GEWA SE; (d) Turbo-B.

$(T_w - T_s)$ was converted to temperature units using the NBS calibration, with the cold junction at the saturation temperature. The measured wall temperature was extrapolated to the base of the fins for each tube geometry using the heat conduction equation in cylindrical coordinates. The wall thermocouple junction is located at the bottom of the groove, approximately 0.60 mm below the root diameter of the tube.

The apparatus also has a charging line, a discharging line, an evacuating line connected to a positive displacement vacuum pump, and a connection to

Table 1. Dimensions of tube tested

Tube	GEWA K26	GEWA TX19	GEWA SE	Turbo-B
D_o (mm)	18.8	17.5	18.0	19.1
Fins/in. (in.$^{-1}$)	26	19	27	42
Fin height (mm)	1.46	0.85	1.03	0.62
Fin gap (mm)	—	0.14–0.20	0.16–0.20	0.10–0.18
Notch depth (mm)	—	0.11*	0.06*	0.20†
Notch pitch (mm)	—	0.97*	1.05*	0.77†
Figure	1(a)	1(b)	1(c)	1(d)

* Notches in the wall between fins.
† Notches in the fins, parallel to tube axis.

read the boiler pressure. Depending on the magnitude of the pressure, it was read using either a U-tube mercury manometer, or a pressure transducer calibrated by a dead-weight tester. The condenser was cooled by city water for the 27°C tests, and by 1.1°C aqueous ethylene glycol for the 4.4°C tests.

EXPERIMENTAL PROCEDURE

Before charging the system, it was evacuated using a vacuum pump. When the system pressure decreased to 27.6 kPa, the system was charged with refrigerant. Before an experiment was started, the pool temperature was compared to the saturation temperature corresponding to the measured saturation pressure. The system was re-evacuated and re-charged or vented to remove air until the agreement was in the range 0.1–0.2 K. A maximum power of 475 W was then supplied to the system, and boiling occurred for one hour before data were taken. The data were taken in order of decreasing power input, starting at 475 W. Data were usually taken to a minimum power input of 25 W. The mass flow rate of the condenser coolant was adjusted at each power input, to maintain constant system pressure. The saturation temperature was maintained at 26.7 ± 0.3°C or 4.4 ± 0.3°C.

The data taken at each power input included the following.

1. Voltage and current to calculate the test section power input.

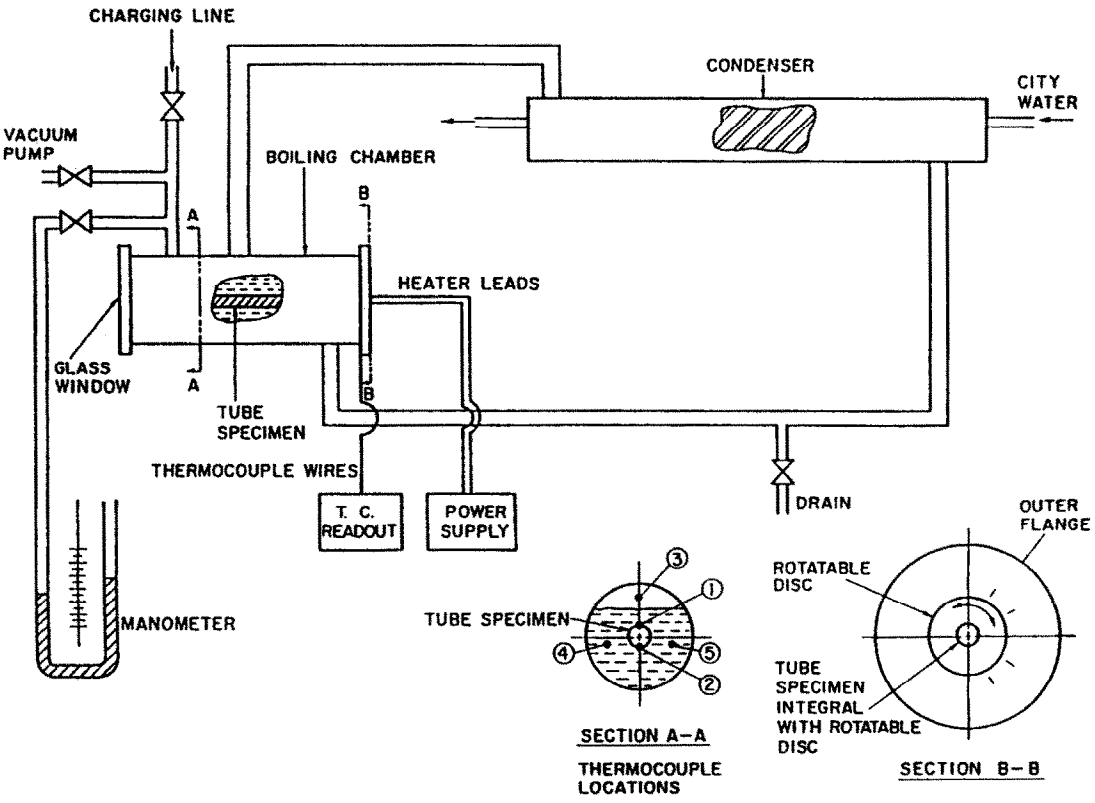

FIG. 2. Schematic of pool boiling test facility.

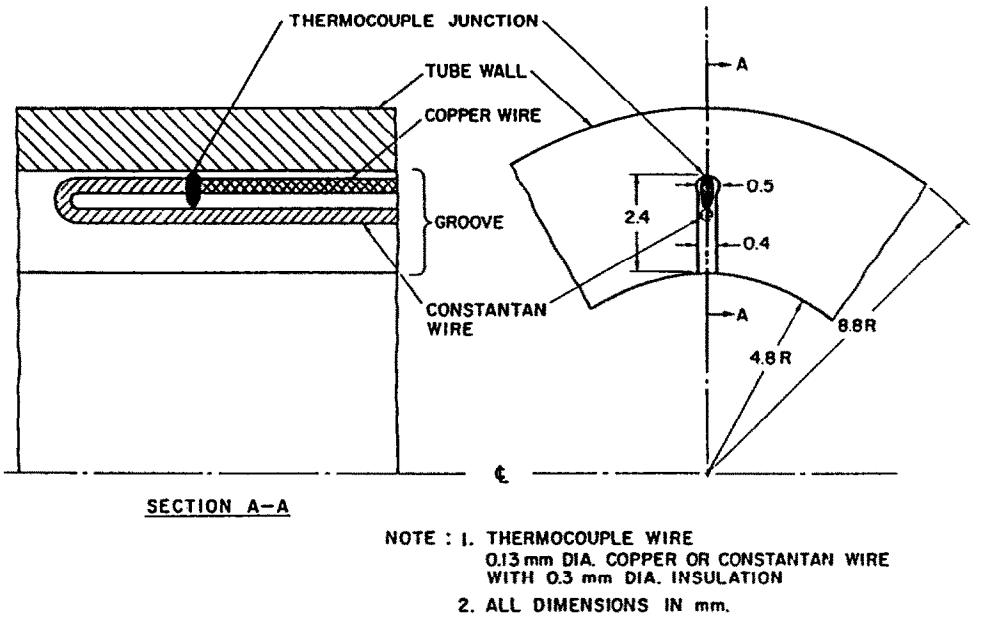

FIG. 3. Illustration of wall thermocouple installation.

2. Readings from both wall thermocouples at angular locations between 0 and 180 degrees in intervals of 30 degrees.

3. The refrigerant temperature and the boiling pressure.

Certain precautions were taken to ensure accuracy in the measurements.

1. The pool temperature was compared to the saturation temperature corresponding to the measured saturation pressure. This ensures that there are no noncondensibles in the system. It also verified that there was no sub-cooling in the liquid pool.

2. The heater was tested for circumferential uniformity of heat flux. This was done by rotating the heater, while keeping the thermocouple locations fixed. Several heaters were tested, and the one that yielded the least variation of thermocouple output was used in the experiments. The wall thermocouple output of this heater did not vary more than 0.05 K when the heater was rotated 360 degrees.

3. The heater was moved 25 mm in the axial direction along the hole. The thermocouple readings varied less than 0.05 K.

4. To validate the thermocouple installation, the tube was rotated, and the temperature was measured at different circumferential locations by the two thermocouples. If these two thermocouples read the same at a given angular location, one concludes that there are no installation errors, and that the heat flux is constant around the heater circumference.

The average wall temperature was used to define the boiling coefficient. It is defined as the average value of the two thermocouples over the six angular positions. This value was then corrected for heat conduction over the 0.6 mm depth between the thermocouple location and root diameter of the fins. The circumferential average wall temperature agreed closely with the average of the wall temperatures at the 0 and 180 degree positions.

The heat flux is based on the heated area of the tube ($\pi D_o L$) where D_o is the envelope diameter over the fins (if present) and L is the heated length of the heater (118 mm).

EXPERIMENTAL ACCURACY

An error analysis was made taking into account the uncertainty associated with the interpolation errors of the measuring devices, the errors due to calibration, and fluctuations in the thermocouple readings during boiling. The heat transfer coefficient was taken as the dependent variable and the heat flux as the independent variable. The nominal uncertainty in the heat transfer coefficient h_{nb} is estimated to be $\pm 8\%$. The major contribution to the uncertainty is the fluctuations in the thermocouple readings for a fixed value of the heat flux. The magnitude of the fluctuation varied from tube to tube and generally decreased with decreasing heat flux. The fluctuations varied from a maximum of 0.4°C for the integral-fin tube to almost no fluctuations for the enhanced tubes. The fluctuations are due to the dynamic nature of boiling. A time-averaged value for $(T_w - T_s)$ was therefore taken at each heat flux. For each heat flux, $(T_w - T_s)$ was averaged over a 5 min period with sampling done every 30 s.

The two liquid pool thermocouples and the vapor

space typically agreed within 0.1°C. The saturation temperature at the measured pressure typically agreed within 0.15°C.

TEST RESULTS

Circumferential variation of $(T_w - T_s)$

Figure 4 shows the variation of wall superheat with angular location for the three different tubes using R-11 at 80°F (27°C) and 60 kW m^{-2} heat flux. This is shown for both wall thermocouples, TC1 and TC2. Figure 4 shows that the circumferential variation of $(T_w - T_s) = \Delta T_{ws}$ has a different trend for the three geometries. This is distinguished by comparing the values of ΔT_{ws} at the top and bottom of the tube. The GEWA K26 tube has a larger ΔT_{ws} at the top than at the bottom, while the opposite is true for the GEWA SE tube. The ΔT_{ws} of the Turbo-B is constant around the circumference. The circumferential variation of ΔT_{ws} is a consequence of the circumferential variation of the local boiling coefficient. Because of the thick tube wall, non-uniform circumferential outer wall temperatures will cause a redistribution of the surface heat flux. For example, the heat flux at the top of the GEWA K26 tube is less than that at the bottom. Thus, the difference of the local heat transfer coefficients at the top and bottom of the GEWA K26 tube is greater than indicated by the local ΔT_{ws} values shown on Fig. 4.

One would expect TC1 and TC2 to show the same temperature at the same angular location. The Turbo-B and the GEWA SE tube showed approximately equal readings for the two thermocouples at the all angular locations. However, TC1 and TC2 differ as much as 0.5 K with angular location for the GEWA K26 integral-fin tube. Both TC1 and TC2 showed a smaller superheat at the bottom of the tube than at the top. This is consistent with results obtained by McKee and Bell [7] who boiled an R-113–oil mixture on a 19 fpi integral-fin tube.

In an attempt to obtain closer agreement between TC1 and TC2 at the same angular location, the thermocouples were removed and reinstalled in the same location. The same behavior still persisted. Then, the thermocouples were once again reinstalled, but at a different axial location. This reinstallation still exhibited a difference between the two wall thermocouple readings at the same circumferential location. The thermocouples used for the different installations were not the same but were made from the same roll of wire. Figure 5 shows the R-11 test results for the GEWA K26 tube, based on averaging TC1 and TC2 at the same angular location. For $q_{nb}/A > 15$ kW m^{-2}, the test results agree very closely.

Non-uniform circumferential heat flux of the heater was ruled out, since the thermocouple readings did not change when the angular location of the ther-

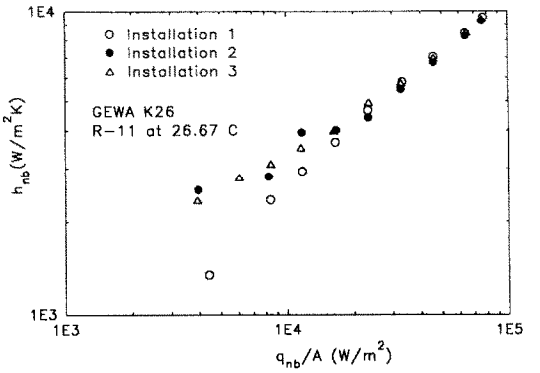

FIG. 5. GEWA K26 results for three different thermocouple installations.

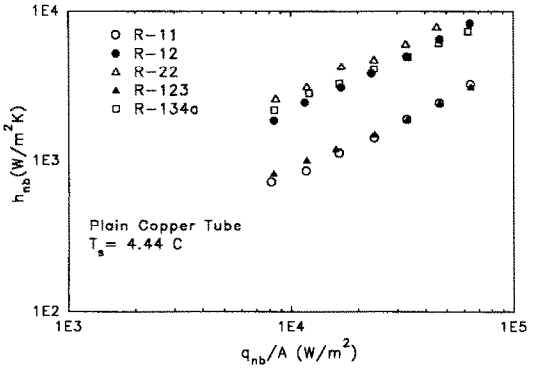

FIG. 6(a). Plain tube data for $T_s = 4.44$°C.

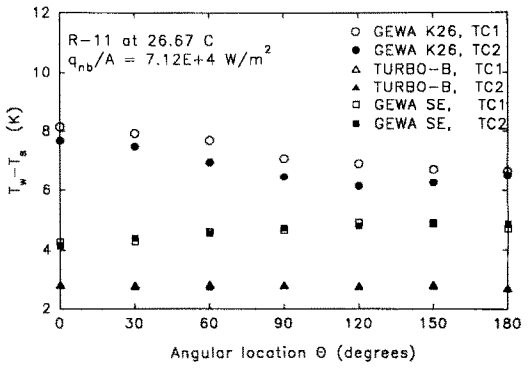

FIG. 4. Variation of $(T_w - T_s)$ with angular location.

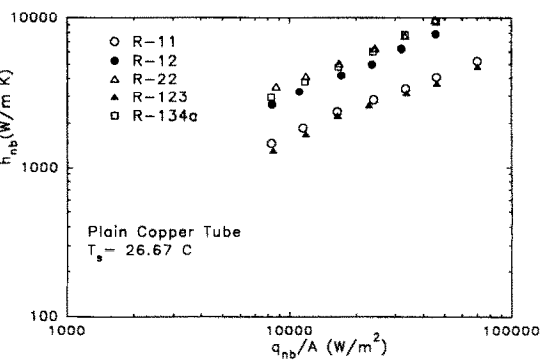

FIG. 6(b). Plain tube data for $T_s = 26.7$°C.

mocouples was held constant, and the heater was rotated. The depth of the grooves was not significantly different, so the temperature drop in the tube wall was also ruled out as a possible explanation. A possible explanation for the anomalous behavior of the GEWA K26 tube is a difference in the nucleation characteristics of the surface associated with the thermocouple grooves 1 and 2. Visual inspection of the fin height, and the character of the fin surface did not reveal noticeable differences in geometry. McKee and Bell [7] have reported similar differences in thermocouple readings at angular locations of 90 and 270 degrees for pool boiling on polished, plain stainless steel tubes in water. If geometrical factors alone governed boiling, these two thermocouples should read the same since they are at geometrically similar locations.

The differences between thermocouple readings are most probably because of different local boiling characteristics at the two thermocouple positions. Hence, the values of each thermocouple at a given angular location were averaged. The results shown in the later figures are presented in this manner.

Pool boiling data

The data for the five tube geometries and five refrigerants are presented in the form of h_{nb} vs q/A on Figs. 6 through 11 and in the Appendix. Each geometry data set is presented in two plots; one for the 4.4°C data and a second for the 26.7°C data. An index to these figures is given in Table 2.

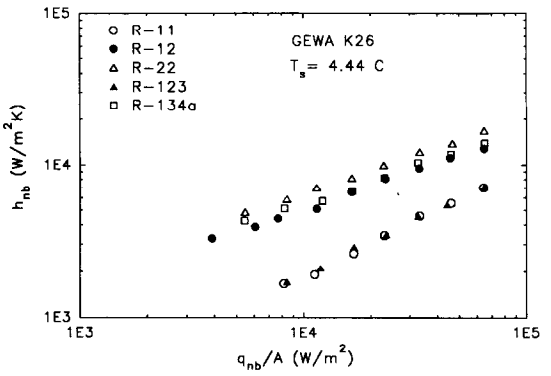

FIG. 7(a). GEWA K26 tube data for $T_s = 4.44$°C.

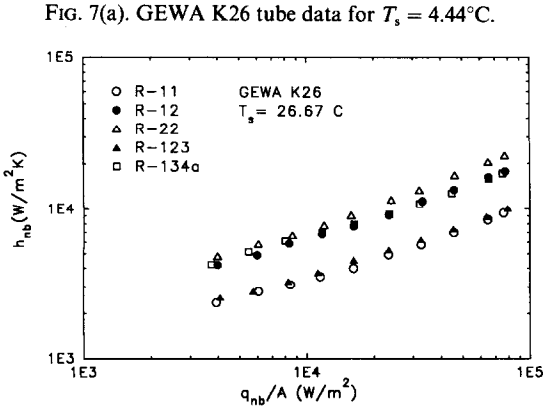

FIG. 7(b). GEWA K26 tube data for $T_s = 26.7$°C.

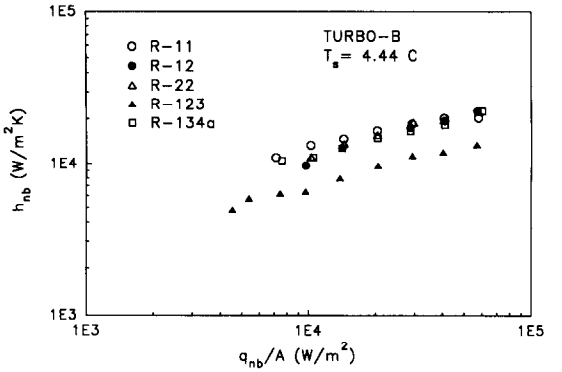

FIG. 8(a). Turbo-B tube data for $T_s = 4.4$°C.

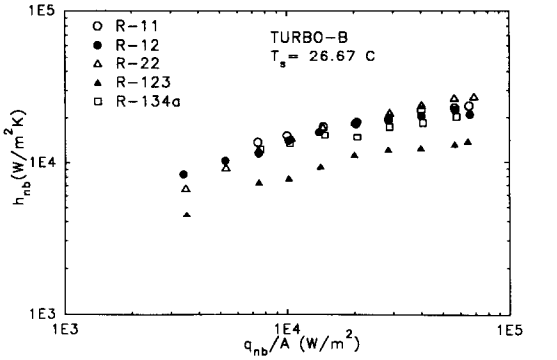

FIG. 8(b). Turbo-B tube data for $T_s = 26.7$°C.

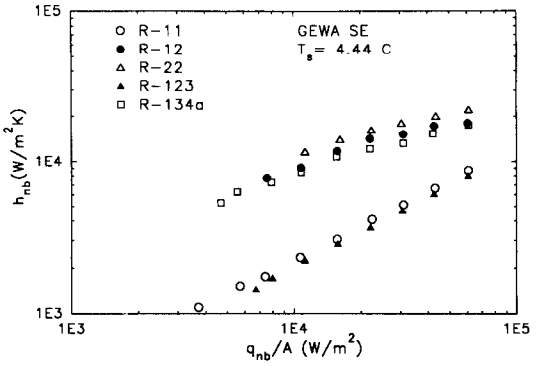

FIG. 9(a). GEWA SE tube data for $T_s = 4.4$°C.

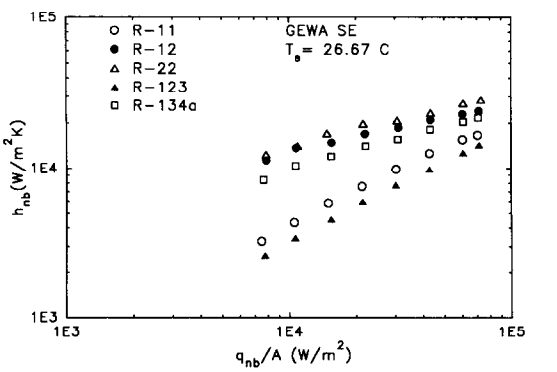

FIG. 9(b). GEWA SE tube data for $T_s = 26.7$°C.

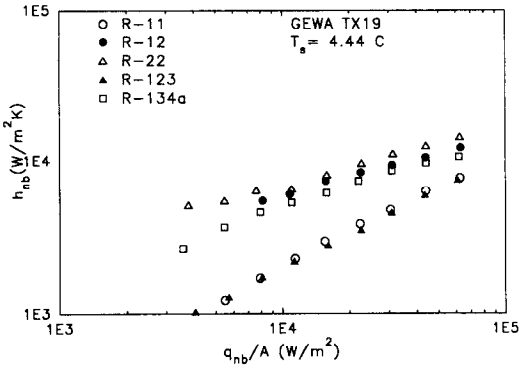

FIG. 10(a). GEWA TX19 tube data for $T_s = 4.4°C$.

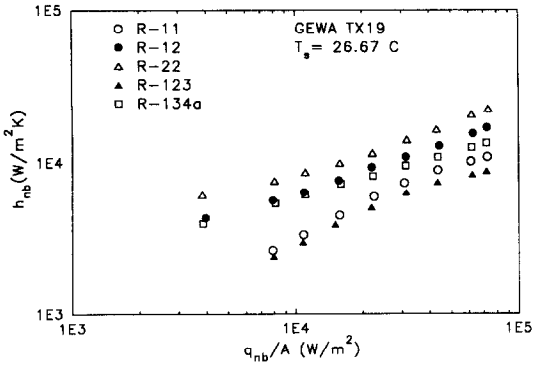

FIG. 10(b). GEWA TX19 tube data for $T_s = 26.7°C$.

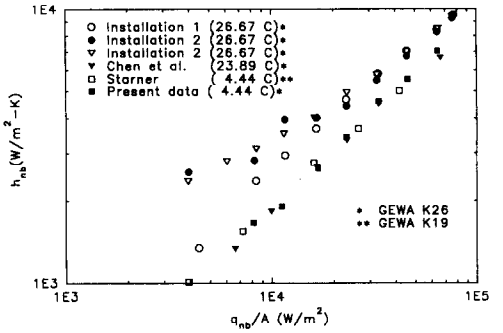

FIG. 11. Comparison of GEWA K26 R-11 with Chen *et al.* [8] and Starner [9].

Table 2. Index to data figures

Geometry	Figure number	
	4.4°C Data	26.7°C Data
Plain	6(a)	6(b)
GEWA K26	7(a)	7(b)
Turbo-B	8(a)	8(b)
GEWA SE	9(a)	9(b)
GEWA TX19	10(a)	10(b)

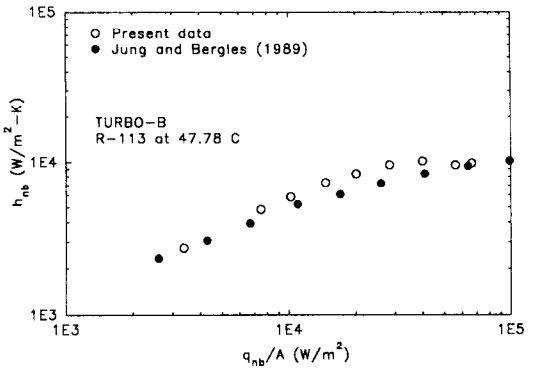

FIG. 12. Comparison of Turbo-B R-113 test results with Jung and Bergles [10].

COMPARISON OF DATA WITH PUBLISHED RESULTS

It is of interest to compare the present data with measurements taken by others. However, the survey of Pais and Webb [6] shows that there are very little published data that may be compared. Figure 11 shows the R-11 test results for the GEWA K26 tube for all three sets of thermocouple installations. The boiling coefficients are approximately 20% higher than the R-11 values measured by Chen *et al.* [8] for a GEWA K26 tube at 24°C (75°F). Also shown on Fig. 11 are 4.4°C R-11 data measured on a 19 fpi tube by Starner [9]. Comparison of the present 40°F GEWA K26 data shows that it is approximately equal to Starner's 19 fpi data.

Figure 12 compares at 1.0 atm the R-113 Turbo-B data with those obtained by Jung and Bergles [10]. Both tubes were made by Wolverine in the same processing batch and had a 6.35 mm inside diameter. The presently tested tube was rebored to 9.53 mm. The Jung and Bergles data fall 0–20% below the present data. They based the heated length on the cartridge length (101.6), rather than the actual heated length of 85.7 mm. Correction of their data to the 85.7 mm

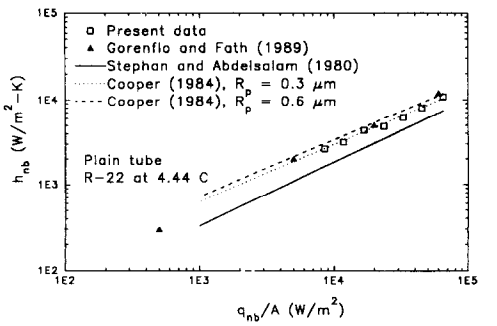

FIG. 13. Comparison of R-22 plain tube data with Gorenflo and Fath [11] and correlations of Cooper [12] and Stephan and Abdelsalam [13].

actual heated length will shift their boiling curve upward approximately 5%.

Figure 13 compares the plain tube R-22 data at 4.4°C with that of Gorenflo and Fath [11]. The present data are 5–10% below that of Gorenflo and Fath. Figure 13 also shows the boiling coefficients predicted by the Cooper [12] and the Stephan and Abdelsalam [13] correlations. Both the present data and those of Gorenflo and Fath [11] fall between the two correlations. The Cooper correlation, shown in equation (2) below, includes the term R_p to account for the micro-roughness of the surface

$$h_{nb} = 90(q'')^{0.67} M^{-0.5} p_r^m (-\log_{10} p_r)^{-0.55} \quad (2)$$

where $m = 0.12 - 0.2 \log_{10} R_p$.

The roughness term, R_p, is the surface roughness expressed in μm. The actual roughness of the commercial finish copper tubes was not measured. Stephan and Abdelsalam [13] report that commercial finish copper tubes have $R_p \simeq 0.4$ μm. The Cooper correlation is shown in Fig. 13 for $R_p = 0.3$ and 0.6 μm roughnesses. The present data agree very closely with the Cooper correlation for $R_p = 0.3$ μm. The Stephan and Abdelsalam correlation under predicts the data 20–25%.

DISCUSSION OF PRESENT RESULTS

Plain tube data

The Cooper [12] correlation contains the parameter p_r and shows that the boiling coefficient increases with increasing p_r. Table 3 lists the critical pressure (p_{cr}), molecular weight (M), and $p_r = p/p_{cr}$ for the five refrigerants tested. The refrigerants are listed in order of decreasing p_r for the 4.4°C condition. Note that the molecular weight decreases as one goes down the table.

Table 3 shows that R-11 and R-123 were tested at the lowest p_r and that their p_r values are equal. Similarly, R-12 and R-134a were tested at approximately equal values of p_{cr}, and their p_r at 4.4°C are approximately eight times that of the R-11 and R-123. The R-22 has the highest p_{cr} and p_r. According to the Cooper [12] correlation, the boiling coefficient of R-123 is 5% below that of R-11, and the boiling coefficient of R-134a is within 1% that of R-12. The Cooper equation shows that boiling coefficients decrease in the order R-11/123, R-12/134a, R-22.

Table 3. Properties and operating conditions of the refrigerants tested

Refrigerant	M	p_{cr} (MPa)	p_r 4.4°C	p_r 26.7°C
R-123	152	3.68	0.011	0.027
R-11	137	4.41	0.011	0.027
R-134a	102	4.06	0.085	0.172
R-12	120	4.12	0.087	0.166
R-22	86	4.99	0.115	0.219

Table 4 shows the ability of the Cooper [12] ($R_p = 0.3$ μm) and Stephan–Abdelsalam [13] correlations to predict the 4.4°C and 26.7°C plain tube data for all five refrigerants. The present plain tube data are well predicted by the Cooper [12] correlation using $R_p = 0.3$ μm. The average error for all of the data is 6.2% over prediction. The Stephan and Abdelsalam [13] correlation tends to under predict the plain tube data. The average error for all of the data is 23% under prediction.

Enhanced tube data

Examination of Figs. 7 through 11 shows that enhanced tubes show the same relative order of boiling coefficients as for the plain tubes, with one exception. The exception is R-11 boiling on the Turbo-B. The Turbo-B R-11 data are substantially higher than those of R-123, and are approximately equal to the R-12 data. This is true for both the 4.4 and 26.7°C data sets. The Turbo-B data appear to be an anomaly. The 4.4°C Turbo-B data were repeated for R-11 and R-22. Both sets of data very closely approximated the original data sets. It is unclear why the R-11 data appear to be inconsistent with the data sets for the other geometries.

The heat flux exponent

The Cooper [12] correlation (equation (2)) shows that the slope of the h_{nb} vs q'' curve should be 0.67, independent of heat flux. Examination of all the data sets shows that the slope of the h_{nb} vs q'' curve is not equal for the various refrigerants. This is much more noticeable for the enhanced tubes than for the plain tubes. Gorenflo [14] and Sokol *et al.* [15] have tested a large number of refrigerants boiling on plain tubes and found that the heat flux exponent is not constant. They plotted their data in the form

$$h_{nb}/h_{nb,o} = c_3(q''/q''_o)^n \quad (3)$$

where

$$n = 0.9 - 0.3(p_r)^{0.3} \quad (4)$$

and q''_o and $h_{nb,o}$ are the heat flux and boiling coefficient, respectively, at a reference heat flux of 20 kW m^{-2}.

Curve fits of the Figs. 6(a) and 10(a) data at 4.4°C yield the heat flux exponents shown in Table 5 for the plain and GEWA TX19 surfaces. Table 5 shows that the heat flux exponent of the present plain tube data reasonably agree with equation (2). The present GEWA TX19 data show a smaller heat flux exponent than does the GEWA TX19 data of Gorenflo *et al.* [16]. Table 5 shows that operation of plain tubes at higher p_r result in smaller heat flux exponents.

If the same trends existed for the enhanced tubes, one would expect R-11 and R-123 to have higher slopes than for R-12, R-123 and R-22. This is based on the values of p_r given in Table 5. The R-22 should

Table 4. Ability of correlations to predict plain tube data ($q'' = 30$ kW m^{-2})

Refrigerant	$T_s = 4.4$°C			$T_s = 26.7$°C		
	h_{exp}	h_C/h_{exp}	$h_{S\&A}/h_{exp}$	h_{exp}	h_C/h_{exp}	$h_{S\&A}/h_{exp}$
R-11	1790	1.09	0.78	3190	0.84	0.61
R-123	1830	1.00	0.90	2920	0.91	0.84
R-12	4770	0.96	0.75	5990	1.05	0.84
R-134a	4770	1.04	0.77	7130	0.97	0.72
R-22	6040	1.02	0.69	7370	1.18	0.82

have the smallest slope. Examination of Figs. 6 through 10 shows that this is true for all geometries, except the R-11 boiling on the Turbo-B.

Performance comparison of the competing refrigerants

It is intended that R-123 replace R-11, and R-134a replace R-12. It is interesting to compare the boiling coefficient of the R-123 with that of R-11, and R-134a with that of R-12. Table 6 shows the ratio of the boiling coefficients (R-123-to-R-11, and R-134a-to-R-12) for 35 kW m^{-2} for the five surface geometries. The tabled ratios are determined from the data points, not curve fitted results.

Except for the Turbo-B, Table 6 shows that the R-123 boiling coefficients are 2% higher-to-7% lower than those of R-11 on the same surface geometries. Also, for R-134a, Table 6 shows that the R-134a boiling coefficients are 6% higher-to-9% lower than those for R-12 on the same surface geometries. The same boiling coefficient ratios were calculated for the 26.7°C data, and the ratios were consistent with those for the 4.4°C data, including the Turbo-B R-123/R-11 data. Hence the Turbo-B anomaly is consistent at both 4.4 and 26.7°C.

It appears that the R-11 data for the Turbo-B are too high. As previously stated, the Turbo-B R-11 data were repeated and found to be consistent with the original data.

It appears that R-123 and R-134a may replace R-11 and R-12 without any significant performance loss for *nucleate boiling* at 4.4°C on all of the tubes, except for the Turbo-B operating with R-11. One should not immediately conclude that the same boiling coefficient ratios would be obtained in *forced convection* boiling. This is because nucleate boiling may not dominate the forced convection boiling process. Equation (1) contains two terms. The first term involves nucleate boiling, and the second term involves forced convection. Hence, the fluid properties affecting forced convection boiling are also involved. Webb *et al.* [3] have shown that forced convection tends to dominate the forced convection boiling process with standard integral-fin tubes.

For the high performance enhanced tubes (GEWA TX19, GEWA SE, and Turbo-B) nucleate boiling will dominate the performance. It is likely that this conclusion will also be applicable to forced convection boiling in actual chiller operation, because nucleate boiling should dominate equation (1) for 'enhanced' tubes. This was shown for R-11 by the analysis of Webb and Apparao [4]. Assuming the anomaly observed for the Turbo-B tube with R-11 is correct, one would expect an approximate 40% reduction of the shell side coefficient when R-123 replaces R-11 on the Turbo-B tube.

Table 5. Heat flux exponents at 4.4°C

Refrigerant	p_r	Exponent		
		Plain (Exp)	Plain (Eqn (2))	GEWA TX19 (Exp)
R-11	0.011	0.74	0.82	0.78
R-123	0.011	0.65	0.82	0.73
R-12	0.088	0.72	0.75	0.39
R-134a	0.085	0.60	0.76	0.42
R-22	0.343	0.68	0.68	0.39

Table 6. Comparison of boiling coefficients at 4.4°C and $q'' = 35$ kW m^{-2}

Geometry	Boiling coefficient ratio	
	R-123/R-11	R-134a/R-12
Plain	1.02	1.00
GEWA K26	0.96	1.06
GEWA TX19	0.95	0.91
GEWA SE	0.93	0.91
Turbo-B	0.60	0.98

CONCLUSIONS

1. Pool boiling data are provided at 40°F (4°C) and 80°F (27°C) for five refrigerants boiling on a plain tube, a GEWA K26 integral-fin tube, and three enhanced tubes.

2. The pool boiling coefficients for alternate refrigerants R-123 and R-134a are within 10% of the values for R-11 and R-12, respectively, for all tubes, except the Turbo-B with R-11/123.

3. Except for the Turbo-B R-11/R-123 data, the data show that approximately equal boiling coefficients will be obtained for different refrigerants, if operated at the same p_r.

4. The boiling heat transfer coefficient for a given heat flux increases with an increase in saturation temperature for all tube geometries. This corresponds to operation at increased p_r.

5. The anomaly observed for the Turbo-B tube is

not understood. The R-11 data appear to be higher than can be justified by use of equation (4).

Acknowledgements—This work was partially sponsored by ASHRAE as RP-392. TC-8.5 monitored the program under the Chairmanship of Mr Petur Thors. Additional funding, and the GEWA K26, the GEWA TX and the boiling tubes were provided by Wieland-Werke, Ulm, F.R.G. The Turbo-B tube was provided by Wolverine Tube, Inc., Decatur, AL.

REFERENCES

1. J. C. Chen, A correlation for boiling heat transfer to saturated fluids in convective flow, *6th National Heat Transfer Conference*, ASME Paper 63-HT-34, Boston, MA (1963).
2. R. L. Webb, K.-D. Choi and T. R. Apparao, A theoretical model for prediction of the heat load in flooded refrigerant evaporators, *ASHRAE Transactions* **95**, 326–348 (1989).
3. R. L. Webb, T. R. Apparao and K.-D. Choi, Prediction of the heat duty in flooded refrigerant evaporators, *ASHRAE Transactions* **95**, 339–348 (1989).
4. R. L. Webb and T. R. Apparao, Performance of flooded refrigerant evaporators with enhanced tubes, *Heat Transfer Engng* **11**, 30–44 (1990).
5. United Nations, Montreal Protocol on Substances that Deplete the Ozone Layer—Final Act, United Nations Environmental Program, New York (1990).
6. C. Pais and R. L. Webb, Literature survey on single-tube pool boiling on enhanced surfaces, *ASHRAE Transactions* **97**, 79–89 (1991).
7. H. R. McKee and K. J. Bell, Forced convection boiling from a cylinder normal to the flow, *Chem. Engng Prog. Symp.* **65**, 222–230 (1968).
8. Q. Chen, B. Windisch and E. Hahne, Pool boiling heat transfer on finned tubes, *Eurotherm No. 8—Advances in Pool Boiling Heat Transfer*, Paderborn, F.R.G., pp. 126–141 (1989).
9. K. E. Starner, Private communication with R. L. Webb, Pennsylvania State University, University Park, PA (1988).
10. C. Jung and A. E. Bergles, Evaluation of commercial enhanced tubes in pool boiling, Department of Energy Report No. DOE/ID 12772-1 (1989).
11. D. Gorenflo and W. Fath, Heat transfer on the outside of finned tubes at high saturation pressures, *Proc. XVII Int. Congress of Refrigeration*, Vol. B, pp. 955–960 (1987).
12. M. G. Cooper, Saturation nucleate, pool boiling—a simple correlation, *Int. Chem. Engng Symp. Ser.* **86**, 785–792 (1984).
13. K. Stephan and M. Abdelsalam, Heat transfer correlations for natural convection boiling, *Int. J. Heat Mass Transfer* **23**, 73–87 (1980).
14. D. Gorenflo, *VDI-Wärmeatlas*, Abschnitt HA: Behältersieden, 5. VDI, Dusseldorf (1988).
15. P. Sokol, P. Blein, D. Gorenflo, W. Rott and H. Schömann, Pool boiling heat transfer from plain and fined tubes to propane and propylene, *Heat Transfer 1990: Proc. 9th Int. Heat Transfer Conf.*, Vol. I, pp. 75–80 (1990).
16. D. Gorenflo, P. Blein, W. Rott, H. Schömann and P. Sokol, Pool boiling heat transfer from a GEWA-TX finned tube to propane and propylene, *Eurotherm No. 8—Advances in Pool Boiling Heat Transfer*, Paderborn, F.R.G., pp. 116–126 (1989).

APPENDIX

Curve fit data for pool boiling data

Curve fits of the experimental data were developed in the form $h_{nb} = c(q_{nb}/A)^n$. The table below provides values of the coefficient, c, and the exponent, n.

		$T_s = 4.44°C$		$T_s = 26.67°C$	
Tube	Refrigerant	c	n	c	n
GEWA K26	R-11	2.30	0.726	44.16	0.470
	R-12	41.70	0.519	69.71	0.490
	R-22	59.72	0.509	56.71	0.529
	R-123	2.87	0.706	47.34	0.472
	R-134a	60.43	0.489	102.59	0.452
GEWA TX19	R-11	1.50	0.779	8.53	0.646
	R-12	155.79	0.394	78.79	0.476
	R-22	191.11	0.389	133.07	0.451
	R-123	2.35	0.731	12.65	0.591
	R-134a	105.05	0.423	126.02	0.417
GEWA SE	R-11	2.47	0.739	4.92	0.733
	R-12	189.85	0.421	633.58	0.327
	R-22	346.88	0.380	392.21	0.385
	R-123	1.57	0.776	2.85	0.764
	R-134a	172.78	0.421	100.97	0.487
Turbo-B	R-11	830.46	0.298	1531.97	0.249
	R-12	205.98	0.429	646.49	0.326
	R-22	296.57	0.397	200.47	0.452
	R-123	170.21	0.402	274.72	0.361
	R-134a	304.44	0.389	1455.51	0.240
Plain	R-11	0.87	0.740	7.76	0.584
	R-12	2.71	0.725	7.37	0.650
	R-22	5.28	0.683	11.26	0.629
	R-123	2.32	0.647	6.54	0.592
	R-134a	10.23	0.596	6.78	0.675

DONNEES D'EBULLITION NUCLEEE EN RESERVOIR POUR CINQ REFRIGERANTS SUR DES GEOMETRIES EN TUBES LISSES OU AILETTES

Résumé—On présente des données expérimentales pour l'ébullition nucléée en réservoir sur cinq géométries de tube horizontal avec cinq réfrigérants à deux températures de saturation. Ces réfrigérants sont R-11, R-12, R-22, R-123 et R-134a, à des températures de saturation égales à 4,44°C (40°F) et 26,7°C (80°F). Les géométries considérées sont un tube lisse, un tube ailettes intégrales à 1024 ailettes/m et trois géométries de tubes utilisées commercialement (GEWA TX19, GEWA SE et Turbo-B). Le large domaine des données reportées ici est nouveau. On évalue l'aptitude des formules de Cooper et de Stephan–Abdelsalam à représenter les données du tube lisse. La pente de la courbe du coefficient d'ébullition en fonction du flux thermique dépend de ce dernier. On marque un intérêt pour les données du R-123 et du R-134a qui sont destinés à remplacer respectivement le R-11 et le R-12. Sauf pour le Turbo-B avec R-11, les coefficients de transfert pour R-123 et R-134a sont à 10% près ceux du R-11 et R-12 respectivement.

ERGEBNISSE FÜR DAS BLASENSIEDEN VON FÜNF KÄLTEMITTELN AN GLATTEN, BERIPPTEN UND STRUKTURIERTEN ROHRGEOMETRIEN

Zusammenfassung—Es werden Ergebnisse für das Blasensieden von fünf Kältemitteln bei zwei Sättigungstemperaturen an fünf unterschiedlichen horizontalen Rohrgeometrien vorgestellt. Es wurden die Kältemittel R11, R12, R22, R123 und R134a bei Sättigungstemperaturen von 4,44°C (40°F) und 26,7°C (80°F) verwendet. Die untersuchten Rohrgeometrien sind ein glattes Rohr, ein beripptes Rohr mit 1024 Rippen je Meter und drei kommerzielle strukturierte Rohrgeometrien (GEWA TX 19, GEWA SE und Turbo-B). Erstmals in der Literatur wurde ein derartig weiter Parameterbereich untersucht. Die Anwendbarkeit der Gleichungen von Cooper und von Stephan/Abdelsalam zur Berechnung der Ergebnisse für Glattrohre wurde bestätigt. Ferner ergab sich, daß die Steigung der Kurve des Wärmeübergangskoeffizienten über der Wärmestromdichte von letzterer abhängig ist. Von besonderem Interesse sind die Ergebnisse von R123 und R134a, die R11 bzw. R12 ersetzen sollen. Die Wärmeübergangskoeffizienten beim Sieden von R123 und R134a weichen um weniger als 10% von denjenigen für R11 bzw. R12 ab—mit Ausnahme des Rohres Turbo-B mit R11.

ДАННЫЕ ПО ПУЗЫРЬКОВОМУ КИПЕНИЮ В БОЛЬШОМ ОБЪЕМЕ ДЛЯ ПЯТИ ХЛАДАГЕНТОВ НА ПЛОСКИХ ТРУБАХ С ЦЕЛЬНЫМИ РЕБРАМИ, А ТАКЖЕ ТРУБАХ С ПОВЫШЕННОЙ ПРОИЗВОДИТЕЛЬНОСТЬЮ

Аннотация—Приводятся данные по пузырьковому кипению в большом объеме на пяти различных горизонтальных трубах с использованием пяти хладагентов при двух значениях температуры насыщения. Исследовались хладагенты R-11, R-12, R-22, R-123 и R-134a при значениях температуры насыщения, равных 4,44 °C (40 °F) и 26,7 °C (80 °F). Использовались следующие типы труб: гладкая труба, труба с цельными ребрами (1024 ребра/м) и три используемых в промышленности геометрии труб с повышенной производительностью (GEWA TX19, GEWA SE и Turbo-B). Большое количество представленных данных ранее не были опубликованы. Оценивается возможность описания пузырькового кипения в случае гладкой трубы по обобщающим зависимостям Купера и Стефана – Абдельсалама. Найдено, что наклон кривой, представляющей зависимость коэффициента кипения от теплового потока, определяется величиной теплового потока. Особенно важными являются данные по R-123 и R-134a, которые должны заменить соответственно R-11 и R-12. За исключением случая Turbo-B при использовании R-11, коэффициенты кипения для R-123 и R-134a отличны от значений для R-11 и R-12 соответственно не более, чем на 10%.